

## Boundary between the near-Earth ( $<10 R_E$ ) plasma sheet and outer plasma sheet: Equatorial observations at 9–15 $R_E$ by Geotail

Hisato Shirai<sup>1\*</sup>, Tomoaki Hori<sup>2</sup> and Toshifumi Mukai<sup>3</sup>

<sup>1</sup>*Ichinoseki National College of Technology, Hagisyo, Ichinoseki 021-8511*

<sup>2</sup>*National Institute of Information and Communications Technology, Koganei-shi, Tokyo 184-8795*

<sup>3</sup>*Institute of Space and Astronautical Science, Sagami-hara-shi 229-8510*

\*Corresponding author. E-mail: shirai@ichinoseki.ac.jp

(Received December 10, 2004; Accepted January 28, 2005)

**Abstract:** Equatorial observations of a boundary between the near-Earth ( $<10 R_E$ ) plasma sheet and outer plasma sheet in the magnetotail are reported in the present paper. Analyzing energy-time spectrograms of low energy particles obtained by the Geotail spacecraft, we find that there often exists a boundary between the near-Earth plasma sheet and the tail plasma sheet. At this boundary, fluctuating particle spectra in the magnetotail change to stable spectra in the near-Earth region and energy flux of particles increases rapidly. Repeated observations of these signatures suggest that there often exists a spatial boundary between the two regions. In the present paper, we call this boundary “near-Earth plasma sheet boundary (NEPS boundary)” and examine it in detail. We show that the NEPS boundary is located usually at distances of around 9–15  $R_E$  on the night side near the magnetospheric equator. We also discuss a new method of mapping, in which the NEPS boundary is used as a tracer to map auroral regions to the magnetosphere without using field-line models.

**key words:** new boundary, plasma sheet, magnetotail

### 1. Introduction

Recent papers have pointed out importance of the equatorial region of geocentric distances of around 10–15  $R_E$ . Shiokawa *et al.* (1998) have analyzed magnetic field and particle data obtained by six satellites at distances between 5  $R_E$  and 20  $R_E$ . They suggested that braking of earthward plasma flows occurring at the boundary (10–20  $R_E$ ) between dipolar and tail-like field may be a key to solving a discrepancy between substorm onset models; for example, there is a discrepancy between the current disruption model (*e.g.*, Lui, 1991) and the neutral line model (*e.g.*, Hones, 1976). The former explains the onset by tail current disruption beginning in the near-Earth region ( $<10 R_E$ ), while the latter accounts for the onset by formation of magnetic neutral lines in the magnetotail ( $>15 R_E$ ). Delcourt and Belmont (1998) have examined behaviors of ions in the plasma sheet at 8–15  $R_E$  by performing numerical calculations of ion trajectories in the magnetotail. The results indicated that ion behaviors near the equator at distances of around 9–10  $R_E$  are chaotic, and an intense tail current is generated at this distance. Zelenyi *et al.* (2002) have also examined ion behaviors in

the magnetotail and proposed a model of current sheet evolution. In this model, a thin current sheet is formed in the magnetotail and evolves through a positive feedback process. In this process, the tail current producing the thin current sheet is enhanced by non-adiabatic ion motions, and the rate of non-adiabatic ions increases with decreasing thickness of the tail current sheet.

Analyzing auroral particle data obtained at low altitudes is another method to obtain information on physics in the equatorial region of distances of  $10\text{--}15 R_E$ . However, comparison of auroral phenomena with magnetospheric phenomena occurring in this region has been difficult for the following reason. We usually utilize field line models like Tsyganenko models (Tsyganenko, 1987, 1989) for mapping of auroral regions to the magnetosphere (*e.g.*, Weiss *et al.*, 1992). In these models, the field configuration changes from dipolar-like to tail-like field at distances of  $10\text{--}20 R_E$  rapidly and thus the projection on the equatorial region of  $10\text{--}20 R_E$  highly depends on the field line models. For this reason, it is difficult to map auroral regions to the magnetosphere without ambiguity due to a large dependence on field line models.

As proposed in later sections, we have another method for mapping in which field-line models are not utilized. It is the mapping using boundary signatures based on particle observations. If we know a boundary observed both at low and high altitudes, we can use it as a tracer. A number of particle boundaries have been discovered at auroral altitudes and in the magnetosphere. Although there is a problem of terminology (*i.e.*, the same boundary is occasionally called by different names), we can mention several of the boundaries in the following way; when a satellite surveys auroral regions from high to low latitudes, it will observe (A1) the polar cap boundary at the high-latitude edge of the auroral oval, (A2) the low-latitude boundary between the velocity-dispersed ion signature (*e.g.*, Saito *et al.*, 1992), (A3) the low-latitude boundary of the ion gap (*e.g.*, Bosqued *et al.*, 1993), (A4) the boundary between the discrete and the diffuse aurora, (A5) the isotropy boundary (Sergeev *et al.*, 1993), (A6) the high-latitude boundary of the ion drop-off band (Shirai *et al.*, 1997), (A7) the low-latitude edge of auroral electron precipitation, and (A8) the low-latitude edge of auroral ion precipitation. This summary of low-altitude boundaries is not complete nor generally accepted but is a list of boundaries which we can find in the E-t spectrograms obtained by the Akebono spacecraft on the nightside auroral region. More comprehensive survey of low-altitude boundaries was made by Newell *et al.* (1996) using the DMSP data with quantitative definitions of boundaries.

On the other hand, when a satellite surveys the magnetosphere, it will observe (B1) the boundary between the lobe and the plasma sheet boundary layer (PSBL), (B2) the boundary between the PSBL and the plasma sheet (*e.g.*, Saito *et al.*, 1998), (B6) the outer boundary of the ion drop-off band (Shirai *et al.*, 1994), (B7) the plasmopause, and (B8) the inner boundary of the plasma sheet (*e.g.*, Kerns *et al.*, 1994). The boundaries A1, A2, A6, A7, and A8 detected at auroral altitudes have been interpreted as the ionospheric projection of the boundaries B1, B2 (*e.g.*, Zelenyi *et al.*, 1990), B6 (Shirai *et al.*, 1994; Yermolaev, 2000), B7, and B8 (*e.g.*, Fairfield and Vinas, 1984) in the magnetosphere, respectively. Since these boundaries are observed at both altitudes, we can utilize the boundaries as tracers and compare auroral phenomena with magnetospheric phenomena observed around these boundaries. Although we found

the boundaries B1, B2, B6–B8 corresponding to the auroral boundaries A1, A2, A6–A8, we have not discovered the magnetospheric boundaries corresponding to the auroral boundaries A3, A4, and A5. Since it is difficult to detect the isotropy boundary (*i.e.*, the boundary corresponding to A5) near the magnetospheric equator because of anisotropy in pitch angle distributions of particles decreasing with increasing altitudes, the boundaries we may find in the magnetosphere are the boundaries corresponding to A3 and A4.

In addition to the low-energy particle boundaries, a high-energy ( $>30$  keV) particle boundary has been found recently at low altitudes of  $3\text{--}4R_E$  using the Cluster spacecraft (Sergeev *et al.*, 2003). The Cluster data indicated that there exists a sharp boundary between the inner magnetosphere and active outer plasma sheet. The inner magnetosphere was filled with a larger flux of high-energy ( $>30$  keV) electrons, and the outer region had a lower ion pressure. The boundary was observed at latitudes of  $64\text{--}65$  degrees, which is mapped to the geocentric distance of about  $10R_E$  near the magnetospheric equator when we utilize the field line model of Tsyganenko 1989. They supposed that the boundary is a short-lived structure as suggested by rare appearance and could be generated by a sudden braking of localized bursty fast flows produced by magnetic reconnection.

In this paper, we report equatorial observations of a boundary between the near-Earth ( $<10R_E$ ) plasma sheet and outer plasma sheet in the magnetotail by Geotail. We propose to interpret this boundary as the field-aligned projection of the low-latitude boundary of the ion gap, that is, the boundary corresponding to A3 stated above.

## 2. Observation

The Geotail spacecraft surveyed the distant magnetotail from 1992 to 1994. After that, its apogee distance was lowered to  $50R_E$  in 1994 and to  $30R_E$  in 1995. The data analyzed in this paper were obtained in 1995 and later years at geocentric distances of around  $9\text{--}30R_E$ . Energy-time (E-t) spectrograms of  $10\text{ eV--}40\text{ keV}$  particles were obtained by the LEP instrument (Mukai *et al.*, 1994).

Figure 1 presents an example of near-equatorial observations by Geotail. E-t spectrograms of ions (top) and electrons (bottom) obtained for the interval from 1100 UT to 2100 UT on June 27, 2002 are shown in two panels. For this interval, the geomagnetic condition was quiet ( $Kp=0+, 1$ ) and any substorm activity was not observed. The Geotail spacecraft surveyed the equatorial magnetosphere near the perigee on this day. The trajectory for this interval is plotted on the  $X_{GSM}\text{--}Y_{GSM}$  plane in Fig. 2. As seen in Fig. 1, the spacecraft was first in the plasma sheet boundary layer (PSBL) or in the lobe (at 1100–1200 UT). The PSBL can be identified by coexistence of velocity-dispersed ion signature in higher-energy range ( $>1\text{ keV}$ ) and a weak flux of cold ions in lower-energy range ( $<1\text{ keV}$ ), which was detected at 1100–1120 UT and 1140–1200 UT. The lobe is characterized by very weak (or no) particle fluxes, which were detected at 1120–1140 UT. After that, the spacecraft observed fluctuating fluxes of ions and electrons until 1830 UT. We can notice that characteristics of particle spectra changed rapidly around 1830 UT. The fluctuation disappeared, and stable particle spectra with intense fluxes appeared around 1830 UT. From the long-term

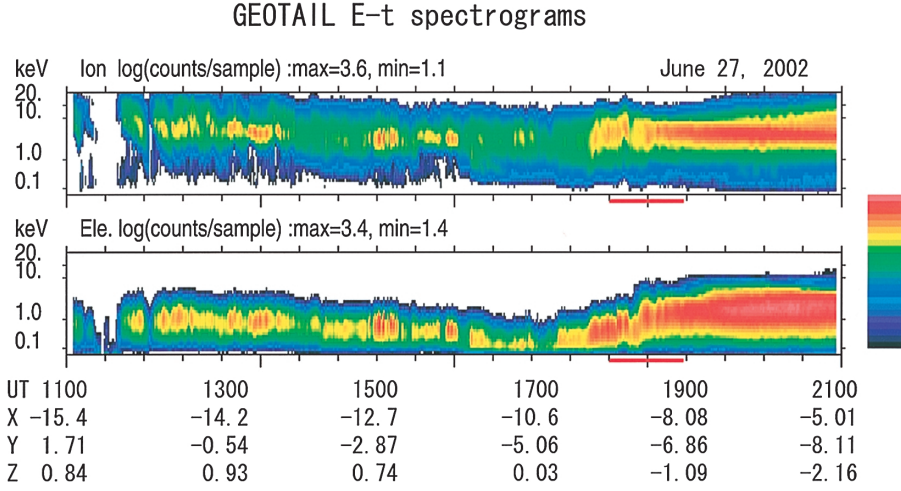


Fig. 1. Geotail observations for the interval of 1100 UT to 2100 UT on June 27, 2002. Energy-time spectrograms of omnidirectional ions (top) and electrons (bottom) show clear changes in particle features between 1800 UT and 1900 UT. A red line below each panel indicates the time interval for which changes are most remarkable.

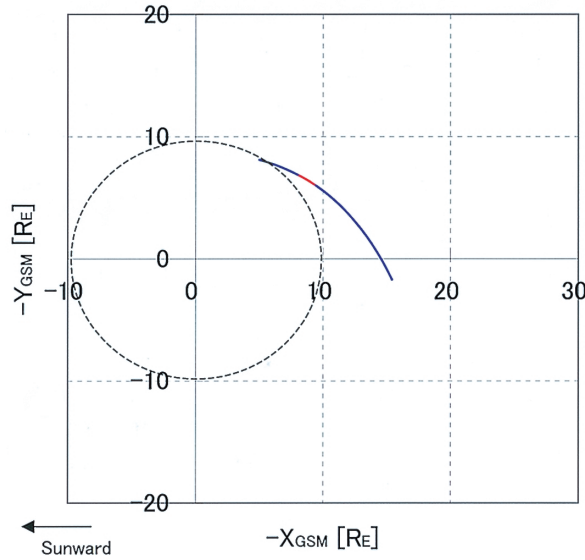


Fig. 2. The Geotail trajectory for the interval of 1100 UT to 2100 UT on June 27, 2002 plotted on the  $X_{\text{GSM}}-Y_{\text{GSM}}$  plane. Geotail crossed the NEPS boundary in the time interval indicated by a red line.

observation performed by Geotail, we have found that this rapid transition is often observed near the perigee of  $9-10 R_E$ . Repeated observations of this signature suggest that there often exists a spatial boundary between the near-Earth plasma sheet and outer

plasma sheet in the magnetotail. We call this boundary “near-Earth plasma sheet (NEPS) boundary” in this paper.

### 3. Position of the NEPS boundary

In order to examine position of the NEPS boundary, we have analyzed the data obtained in three years of 1995–1997 and found 57 crossings of the NEPS boundary by Geotail. The following procedure was utilized for identification of the NEPS boundary. (1) First, we examined whether or not the spacecraft obtained stable particle spectra near the perigee. Flux variation of particles in the near-Earth ( $< 10 R_E$ ) plasma sheet was often so small that we can separate it from a large flux variation in the outer plasma sheet clearly. (2) After we found stable particle spectra, we checked whether the spacecraft surveyed the outer plasma sheet in the magnetotail after/before the perigee observation. We chose only spectral changes occurring between the near-Earth region and the magnetotail but not changes observed at the dayside magnetopause or at the LLBL. (3) After that, we checked whether the changes took place within one hour or more than two hours. When the change took place within one hour, we regarded it as a boundary. Through this procedure, we have identified 57 examples of the NEPS boundary crossings in three-year data of Geotail. The crossing time is defined as the center of the time interval of 60 min for which spectral change is most remarkable.

Figure 3 shows positions of the 57 crossings of the NEPS boundary plotted on the  $X_{GSM}$ - $Y_{GSM}$  plane. As shown in the figure, the NEPS boundary exists usually at 9–15  $R_E$ . It would be noteworthy that the width of the distribution in the radial direction is not very large but narrow especially in the midnight sector. In Fig. 4, the number of

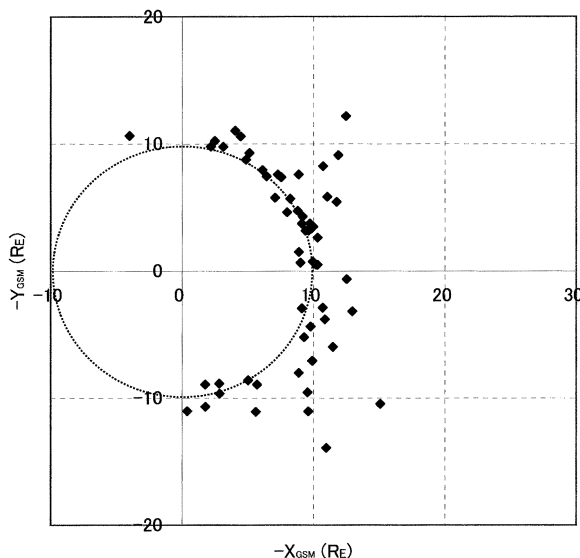


Fig. 3. Position of the NEPS boundary crossings by Geotail. The crossings occurred at distances of 9–15  $R_E$  on the night side.

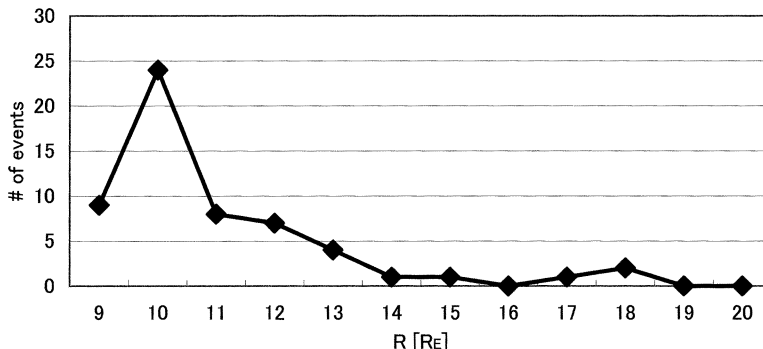


Fig. 4. The distribution of occurrence of the NEPS boundary crossing. The number of occurrence is plotted against the radial distance,  $R = (X_{\text{GSM}}^2 + Y_{\text{GSM}}^2)^{1/2}$ .

occurrence of the NEPS boundary crossings is plotted against the radial distance from the Earth. The positions are mostly distributed in the width of about  $5R_E$  between  $9R_E$  and  $14R_E$ . (The earthward termination of the distribution may be attributable to the limit of coverage of the Geotail observations.)

#### 4. Discussion

This paper has reported equatorial observations of the NEPS boundary. The Geotail data have shown that there often exists a spatial boundary between the near-Earth ( $<9\text{--}15R_E$ ) plasma sheet and outer plasma sheet in the magnetosphere. Firstly, we discuss influence of temporal variability of the plasma sheet on identification of the NEPS boundary. One may suppose that we can observe very fluctuating spectra even near the perigee ( $\sim 9R_E$ ) during substorms, or that we can find prolonged time periods of stable particle spectra near the Geotail apogee ( $\sim 30R_E$ ) during quiet conditions. In fact, we have found several examples in which fluctuating spectra were observed near the perigee. We classified them as examples showing no crossing of the NEPS boundary. On the other hand, we have not found prolonged ( $>4$  hours) time periods of stable particle spectra near the apogee. This result supports our interpretation that the outer ( $>9\text{--}15R_E$ ) plasma sheet is usually variable and is distinguishable from the stable inner plasma sheet.

In order to avoid ambiguity in boundary identification, Newell *et al.* (1996) defined low-altitude particle boundaries quantitatively and investigated the boundary locations. Their study is more precise than previous studies. If we compare our results with theirs, we need to find quantitative criteria for identification of the NEPS boundary. This is a future work of our study.

Secondly, we discuss three boundaries observed at low altitudes as a counterpart of the low-altitude side. One is the low-latitude boundary of the ion gap (*e.g.* Bosqued *et al.*, 1993). The ion gap is a region with very weak ion fluxes in the auroral oval. At the low-latitude boundary of the ion gap, fluctuating particle spectra with very weak fluxes change to stable ones with strong fluxes. The change is very similar to that

occurring at the NEPS boundary. In addition to this similarity, we can point out the following similarity between these boundaries. The low-latitude boundary of the ion gap is observed between the VDIS near the polar cap boundary and the ion drop-off band (IDB) (Shirai *et al.*, 1997). On the other hand, the NEPS boundary is observed between the VDIS in the PSBL and the near-Earth ( $< 9 R_E$ ) magnetosphere, in which IDBs have been detected by Geotail (Shirai *et al.*, 1994) and by Interball (Yermolaev, 2000). From these similarities, we propose that the NEPS boundary is the magnetospheric projection of the low-latitude boundary of the ion gap observed at auroral altitudes.

Another boundary we discuss here is the boundary between the two regions termed “CPS” and “BPS” by Winningham *et al.* (1975). They analyzed the low-altitude satellites, ISIS-1 and 2, to examine electron precipitation on the night side. The electron precipitation region was divided into two regions. One is a relatively stable electron region at lower latitudes, which they call the central region of the plasma sheet (CPS). The other is a higher latitude region with electron structures changing dynamically in response to substorms, which they call the outer boundary layers of the plasma sheet (BPS). Although there is still a terminological problem on these regions due to ambiguity of their definition, their CPS/BPS boundary is often interpreted as the discrete/diffuse auroral boundary. One may suppose that the discrete/diffuse auroral boundary is the field-aligned projection of the NEPS boundary, since fluctuating electron spectra change to stable ones at this boundary. However, this interpretation is not acceptable because the discrete/diffuse auroral boundary does not coincide with the location at which electron energy flux increases rapidly. The latitude of the former is often lower than that of the latter. In order to reveal the association of the NEPS boundary with the discrete/diffuse auroral boundary, we need more thorough study on low- and high-altitude particle boundaries.

The other low-altitude boundary we discuss is the Energetic Electron Wall (EEW) reported by Sergeev *et al.* (2003). In their paper, the EEW was defined as a sudden increase of energetic ( $> 30$  keV) electron fluxes. The thickness of the EEW was estimated to be comparable to the ion gyro-radius of 50 km, which is much smaller than that of the NEPS boundary. This boundary was detected at the latitude of 64–65 degrees, which was expected to be mapped to the distance of about  $10 R_E$  near the equator using the field line model of Tsyganenko 1989. They also reported that an intense Alfvénic wave activity toward the ionosphere was detected on the outside of the EEW, and a gradual increase in ion pressure was observed at the same time as the EEW crossing. These signatures are similar to those of the NEPS boundary. A difference from the NEPS boundary is its rare appearance. The EEW was interpreted as a short-lived structure that could be generated by a sudden braking and azimuthal deflection of localized bursty fast flows produced by the magnetic reconnection in the near tail. Comparing the EEW and the NEPS boundary, we suppose that the field configuration which changes from dipolar to tail-like rapidly at distances of around 9– $15 R_E$  may explain the similar signatures (*i.e.*, a larger fluctuation on the outside and an increase in ion pressure at the boundaries), and substorm activity may account for the difference in the thickness and occurrence frequency. However, we need more detailed analyses of the Geotail and the Cluster data to understand their formation mechanisms.



Finally, we discuss a new method of mapping in which the NEPS boundary and other boundaries are utilized as tracers. As stated in the previous sections, the projection of auroral regions by utilizing field line models highly depends on our choice of models, especially in mapping to the outer ( $>10R_E$ ) equatorial region. Here we propose to use the boundaries observed both at high and low altitudes. The following boundaries can be utilized as tracers; (1) the low-latitude boundary of auroral electron precipitation, which can be mapped to the earthward boundary of plasma sheet electrons and almost corresponds to the plasmopause ( $4-6R_E$ ) (e.g., Fairfield and Vinas, 1984). (2) The high-latitude boundary of the IDB (Shirai *et al.*, 1997) observed at auroral altitudes can be mapped to the outer boundary of the IDB ( $7-9R_E$ ) in the magnetosphere (Shirai *et al.* 1994; Yermolaev, 2000). (3) The VDIS observed near the polar cap boundary has been interpreted as the projection of the VDIS in the PSBL (e.g., Zelenyi *et al.*, 1990). In addition to these boundaries, we can utilize the NEPS boundary as a useful tracer. This boundary would be very helpful for mapping to the outer ( $>10R_E$ ) region, since the method using field line models have a large difficulty especially in mapping to distances larger than about  $10R_E$ , at which the NEPS boundary is observed. Examining the latitude of the Ion Gap boundary and comparing it with the position of the NEPS boundary to obtain the information on the latitudes mapped to the equatorial region of  $9-15R_E$  are left as future works.

## 5. Summary

We can summarize this paper in the following way; (1) we have shown that the Geotail spacecraft often observes a boundary between the near-Earth ( $<10R_E$ ) plasma sheet and outer plasma sheet in the magnetotail. Particle spectra have shown a large flux variation and weak intensity of particles in the outer plasma sheet, while they have a small flux variation and strong intensity in the near-Earth region. We call this boundary “the NEPS boundary”. (2) The statistics using three-year data of Geotail have shown that the NEPS boundary is usually located around  $9-15R_E$ . (3) We have proposed an interpretation that the NEPS boundary is the magnetospheric projection of the low-latitude boundary of the Ion Gap. This interpretation enables us to utilize the NEPS boundary as a helpful tracer for mapping of auroral regions to the outer ( $>10R_E$ ) magnetosphere.

## Acknowledgments

The work was supported by National Institute of Polar Research. The work was also carried out as a joint research program of the Solar-Terrestrial Environmental Laboratory, Nagoya University, and supported by JSPS Grant-in-Aid for Scientific Research (C) 16540409.

The editor thanks Drs. K. Shiokawa and V.A. Sergeev for their help in evaluating this paper.



## References

- Bosqued, J.M., Ashour-Abdalla, M., Alaoui, M.E., Zelenyi, L.M. and Berthelier, A. (1993): AUREOL-3 observations of new boundaries in the auroral ion precipitation. *Geophys. Res. Lett.*, **20**, 1203–1206.
- Delcourt, D.C. and Belmont, G. (1998): Ion dynamics at the earthward termination of the magnetotail current sheet. *J. Geophys. Res.*, **103**, 4605–4613.
- Fairfield, D.H. and Vinas, A.F. (1984): The inner edge of the plasma sheet and the diffuse aurora. *J. Geophys. Res.*, **89**, 841–854.
- Hones, E.W., Jr. (1976): The magnetotail: Its generation and dissipation. *Physics of Solar Planetary Environments*, ed. by D.J. Williams. Washington, D.C., AGU, 559–571.
- Kerns, K.J., Hardy, D.A. and Gussenhoven, M.S. (1994): Modeling of convection boundaries seen by CRRES in 120-eV to 28-keV particles. *J. Geophys. Res.*, **99**, 2403–2414.
- Lui, A.T.Y. (1991): A synthesis of magnetospheric substorm models. *J. Geophys. Res.*, **96**, 1849–1856.
- Mukai, T., Machida, S., Saito, Y., Hirahara, M., Terasawa, T., Kaya, N., Obara, T., Ejiri, M. and Nishida, A. (1994): The Low-Energy Particle (LEP) experiment onboard the GEOTAIL satellite. *J. Geomagn. Geoelectr.*, **46**, 669–692.
- Newell, P.T., Feldstein, T.I., Galperin, Y.I. and Meng, C.I. (1996): Morphology of nightside precipitation. *J. Geophys. Res.*, **101**, 10737–10748.
- Saito, Y., Mukai, T., Hirahara, M., Machida, S. and Kaya, N. (1992): Distribution function of precipitating ion beams with velocity dispersion observed near the poleward edge of the nightside auroral oval. *Geophys. Res. Lett.*, **19**, 2155–2158.
- Saito, Y., Mukai, T. and Teresawa, T. (1998): Kinetic structure of the slow-mode shocks in the Earth's magnetotail. *Perspectives on the Earth's magnetotail*, ed. by A. Nishida *et al.* Washington, D.C., AGU, 103–115.
- Sergeev, V.A., Malkov, M. and Mursula, K. (1993): Testing the isotropic boundary algorithm method to evaluate the magnetic field configuration in the tail. *J. Geophys. Res.*, **98**, 7609–7620.
- Sergeev, V.A., Sauvaud, J.-A., Reme, H., Balogh, A., Daly, P., Zong, Q.-G., Angelopoulos, V., Andre, M. and Vaivads, A. (2003): Sharp boundary between the inner magnetosphere and active outer plasma sheet. *Geophys. Res. Lett.*, **30**, 1799–1802.
- Shiokawa, K., Baumjohann, W., Haerendel, G., Paschmann, G., Fennel, J.F., Friis-Christensen, E., Luhr, H., Reeves, G.D., Russell, C.T., Sutcliffe, P.R. and Takahashi, K. (1998): High-speed ion flow, substorm current wedge, and multiple Pi 2 pulsations. *J. Geophys. Res.*, **103**, 4491–4507.
- Shirai, H., Maezawa, K., Mukai, T. and Kaya, N. (1994): Band-like lack of ions around 10 keV observed by the Akebono and the Geotail satellites. *EOS; Trans.*, **75**, 559.
- Shirai, H., Maezawa, K., Fujimoto, M., Mukai, T., Saito, Y. and Kaya, N. (1997): Monoenergetic ion drop-off in the inner magnetosphere. *J. Geophys. Res.*, **102**, 19873–19881.
- Tsyganenko, N.A. (1987): Global quantitative models of geomagnetic field in the cislunar magnetosphere for different disturbance levels. *Planet. Space Sci.*, **35**, 1347–1358.
- Tsyganenko, N.A. (1989): A magnetospheric magnetic field model with a warped tail current sheet. *Planet. Space Sci.*, **37**, 5–20.
- Weiss, L.A., Reiff, P.H., Hilmer, R.V., Winningham, J.D. and Lu, G. (1992): Mapping the auroral oval into the magnetotail using dynamics explorer plasma data. *J. Geomagn. Geoelectr.*, **44**, 1121–1144.
- Winningham, J.D., Yasuhara, F., Akasofu, S.-I. and Heikkila, W.J. (1975): The latitudinal morphology of 10-eV to 10-keV electron fluxes during magnetically quiet and disturbed times in the 2100–0300 MLT sector. *J. Geophys. Res.*, **80**, 3148–3171.
- Yermolaev, Y.I. (2000): Ion gap locations: INTERBALL/TAILO observations. *Proceedings of International Symposium, From solar corona through interplanetary space, into Earth's magnetosphere and ionosphere: Interball, ISTP satellites, and ground based observations*, 58–59.
- Zelenyi, L.M., Kovrazhkin, R.A. and Bosqued, J.M. (1990): Velocity-dispersed ion beams in the nightside auroral zone: AUREOL 3 observations. *J. Geophys. Res.*, **95**, 12119–12139.
- Zelenyi, L.M., Delcourt, D.C., Malova, H.V. and Sharma, A.S. (2002): “Aging” of the magnetotail thin current sheets. *Geophys. Res. Lett.*, **29**, 1608–1611.